COMPUTATIONAL MODELING OF FLOW, HEAT TRANSFER, AND DEFORMATION IN THE CONTINUOUS CASTING OF STEEL

Brian G. Thomas
Mechanical Engineering, University of Illinois at Urbana-Champaign, IL, USA

Abstract: Further technology improvements to complex mature processes, such as the continuous casting of steel, require a combination of careful laboratory experiments, plant trials on the commercial process, and advanced computational models. As computer power increases, computational models are able to contribute more to the understanding, design, and control of these complex processes. Fluid flow models can now include phenomena such as transient behavior during steady casting, including particle transport, capture and removal. Heat flow models can include interfacial slag layer heat, mass and momentum balances, and nonequilibrium crystallization behavior, and can predict slag structure and friction within the mold. Stress models can now make quantitative predictions such as ideal mold taper and maximum casting speed to avoid problems such as off-corner longitudinal cracks. This work presents recent examples of these models, and their comparison with experimental measurements.
Key words: Computational modeling, continuous casting, turbulent flow, heat transfer, interfacial friction, stress analysis, crack formation

1. Introduction

Understanding and controlling the continuous casting process is important because it may introduce defects such as inclusions and cracks, which persist into the final product, even after many later processing steps. In addition to plant experiments and water models, advanced computational models are increasingly able to generate this understanding. Helped by recent improvements in computer power and software, computational models can simulate a wide range of phenomena ranging including fluid flow, heat transfer, and stress generation. This paper shows recent examples of these from the U. of Illinois Continuous Casting Consortium.

2. Simulations of Fluid Flow in Nozzle and Mold

Three-dimensional turbulent flow and particle motion is being predicted in both the nozzle and mold using the Large Eddy Simulation code, UIFLOW [1]. This approach is more accurate than the standard K-ε turbulence model for transient flows [2], and not as computationally intensive as DNS (direct numerical simulation). An example for a trifurcated nozzle submerged 127mm deep into an 984mm wide x 132 mm thick stainless-steel caster is shown in Figure 1 (model domain) and Figure 2 (typical result) [3]. The velocities compare well with quantitative velocity measurements in a water model of this caster [4].

As shown in Figure 3, the model can simulate the top surface contour in both water model (measured from video frames) and in the actual steel caster (measured by inserting a steel sheet into the mold [5]). The shape follows expectations for a typical double-roll flow pattern. The jets impinging the narrow face wall turn upwards and downwards along the narrow face. The momentum of the upward jet lifts the meniscus by a height that can be approximated with a simple energy balance based on the pressure difference at the meniscus [4]. The surface

contour is similar to that of the water model, except that the slag layer buoyancy increases the magnitude of the variations. Level fluctuations can also be predicted.

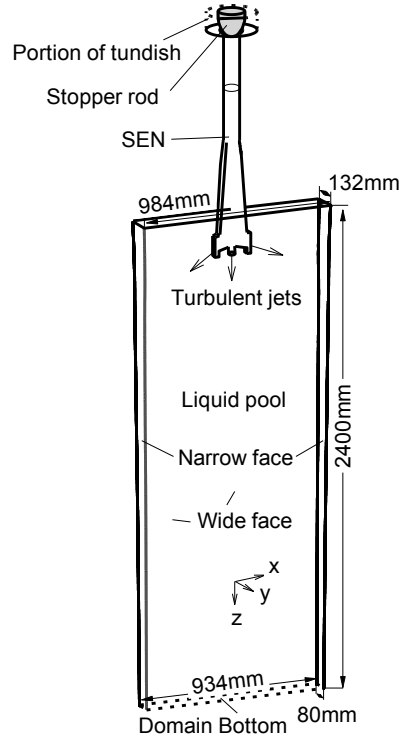

Figure 1. Computational domain of tri-furcated nozzle and thin-slab casting mold

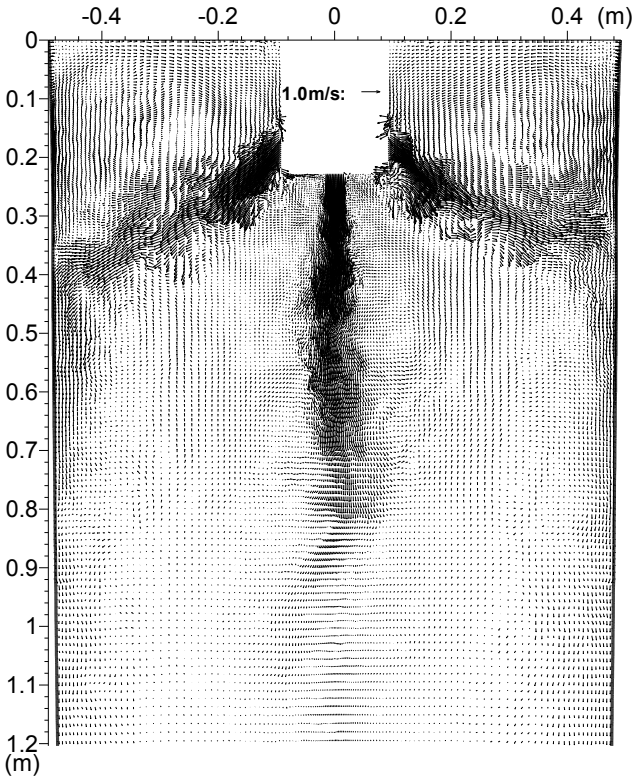

Figure 2. Typical instantaneous velocity vector plot at the center plane between wide faces

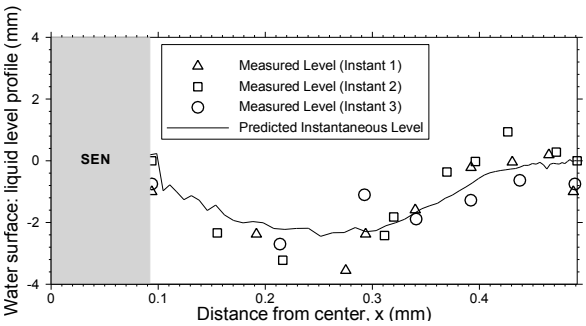

Water model

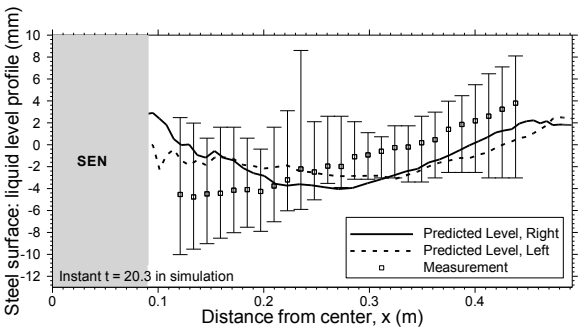

Steel caster

Figure 3. Comparison of predicted and measured top surface liquid levels

The model can also predict the motion of inclusion particles, which can either be entrapped into the solidifying shell to form slivers and cracks, or can be safely removed into the top surface slag layer. Particle transport were simulated using a Lagrangian trajectory-tracking approach, based on the time-dependent flow fields just discussed [6]. The approach was first validated by a successful comparison of transport in a water model where over 50% of the 15,000 particles floated out in 100s. In the actual thin-slab caster, only about 8% of the 40,000 small particles were removed to the top surface [4].

Figure 4 shows a snapshot of the distribution of moving particles in the liquid pool. After a 9s sudden burst of particles entering the steel caster, ~ 4 minutes were needed for all of them to be captured or removed. Note that the particles move with an asymmetrical distribution, in spite of the symmetrical boundary conditions. This is caused by transients in fluid turbulence in the lower recirculation region, rather than by inlet variations at the nozzle port.

The computational results were further processed to predict the ultimate distribution of impurity particles in the solid thin slab after a short burst of inclusions entered the mold [4]. Figure 5 shows that most of the particles end up between 1m below and 1m above the location of the meniscus when they entered the mold. Note that the asymmetric particle distribution during the flow only leads to slight asymmetries in the distribution in the final product. The results were reprocessed to reveal the distribution of total oxygen content for a steady inclusion supply from the nozzle. Figure 6 shows how steel that initially contains 10ppm at the nozzle ports will ultimately range from only 6ppm in the interior to over 50ppm in spots near the narrow face. The greatest inclusion concentration is found near the surface, especially near the narrow faces. Further details are given elsewhere [3, 6]

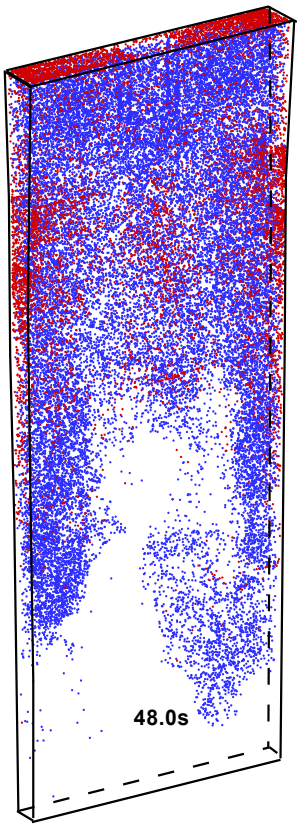

Figure 4. Distribution of moving particles, 48s after injection

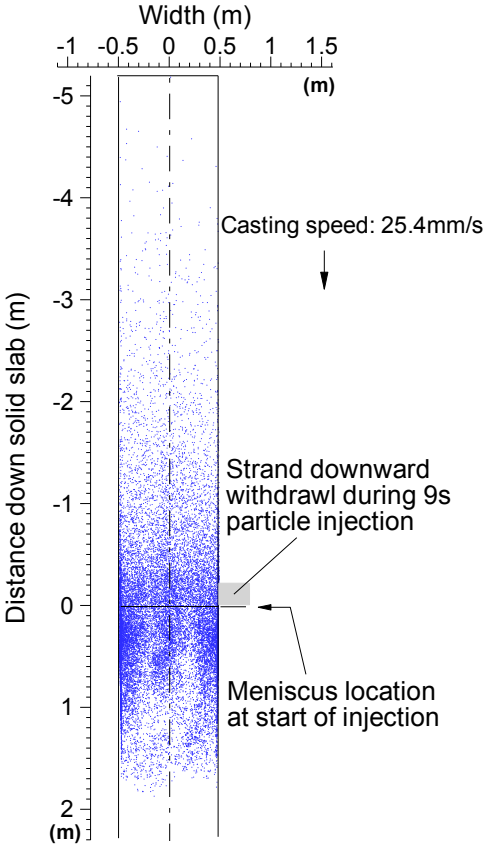

Figure 5. Final entrapment locations for a 9s-burst of particles: view from wide face

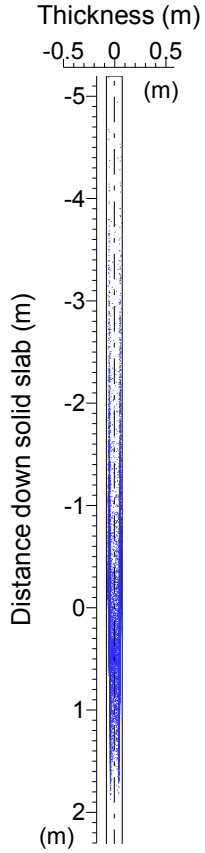

View from narrow face

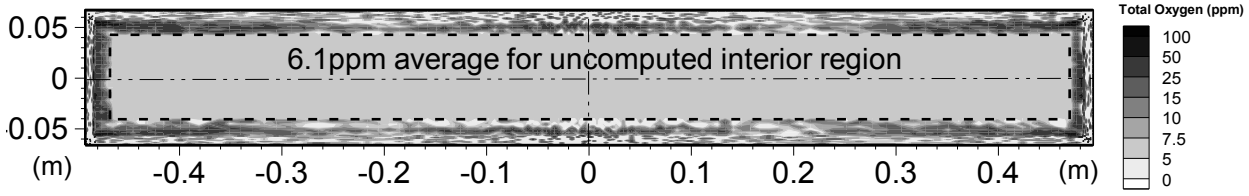

Figure 6. Predicted total oxygen concentration averaged along the slab length

The results of this work confirm the important role of flow transients in the transport and capture of particles during continuous casting, and can serve as a benchmark for future simplified models.

3. Modeling the Mold / Strand Interface

Heat transfer and solidification models are useful for many purposes, including the design of cooling water slots, shell thickness, mold taper, finding the metallurgical length, the design of spray-cooling, and trouble-shooting the location of internal defects (hot tears that form at the solidification front). To study these phenomena, a model (CON1D) has been developed that includes a 1-D transient solidification model in the shell coupled with a 2-D steady model of the model [7]. It features a detailed treatment of the interface between the solidifying strand and the water-cooled mold which governs heat transfer in the process. To investigate mold flux behavior in the gap, the model includes a momentum balance on the solid and liquid flux layers in the gap, and a vertical-direction force balance between friction against the mold wall and shell, and axial stresses in each slice through the solid flux layer (Figure 7). During each oscillation cycle, the model shows (in Figure 8) that the velocity profile in the liquid flux layer varies from the casting speed on the shell side (right) to the mold speed on the solid side attached to the mold wall (left), with a curved profile according the temperature-dependent viscosity of the liquid flux [8]. The accuracy of this part of the model is shown by its matching of results from a finite difference model of flow in the gap.

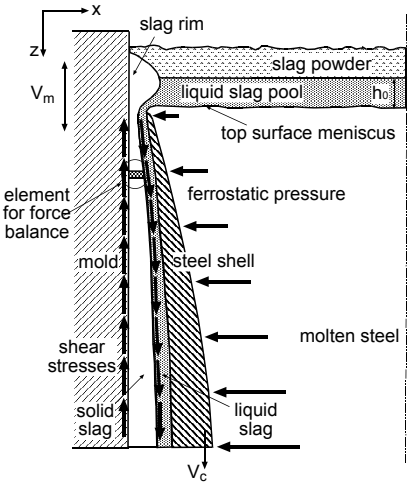

Figure 7 -Schematic of interfacial gap phenomena in continuous casting mold

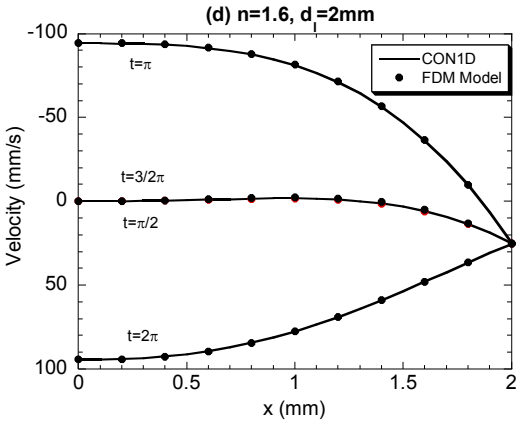

Figure 8 -Velocity profiles in liquid flux layer (for viscosity exponent = 1.6 and film thickness = 2mm)

From the velocity profile and flux consumption, the thermal history and interfacial friction can be predicted in the gap between the shell and mold wall. The mold flux properties change greatly if the flux crystallizes, which is predicted based on the measured TTT diagram [9], as shown in Figure 9. Further details are given elsewhere [8]. .

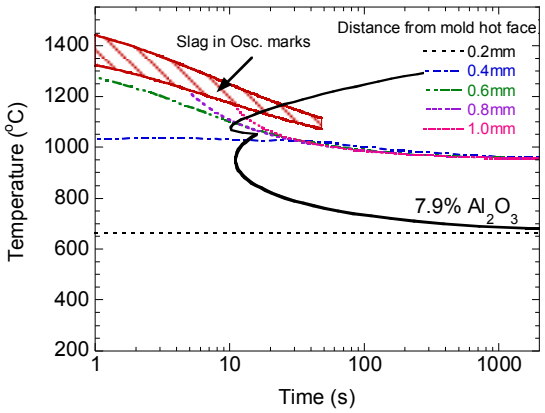

Figure 9 - Slag layer cooling history with attached slag and measured TTT curves

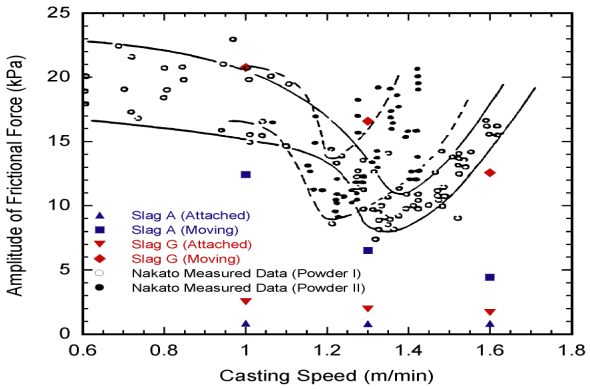

Figure 10 -Effect of casting speed on friction force: measurement and prediction

By integrating the predicted shear stress distribution down the mold over the entire oscillation cycle, the model can predict the total friction force in mold, as shown in Figure 10. It can also be measured in the plant using accelerometers. High in the mold, the flux against the steel shell is molten, so friction is low. Low in the mold, the flux layer may become completely solid, which creates high friction forces. Increasing speed increases the liquid region, thereby lowering friction, which agrees with measurement. At high speed, friction increases due to factors not currently included in the model, such as insufficient taper. This powerful modeling tool can help the interpretation of plant measurements such as friction.
s

4. Stress Modeling of the Solidifying Steel Shell

A coupled finite-element model, CON2D, has been developed to simulate temperature, stress, and shape development during the continuous casting of steel, both in and below the mold [10]. The model simulates a transverse section of the strand in generalized plane strain as it moves down at the casting speed (Figure 11). It includes the effects of heat conduction, solidification, non-uniform superheat dissipation due to turbulent fluid flow, mutual dependence of the heat transfer and shrinkage on the size of the interfacial gap, taper and thermal distortion of the mold. The stress model features an elastic-viscoplastic creep constitutive equation that accounts for the different responses of the liquid, semi-solid, delta-ferrite, and austenite phases. A contact algorithm is used to prevent penetration of the shell into the mold wall due to the internal liquid pressure. An efficient two-step algorithm is used to integrate these highly non-linear equations. The model was validated with analytical solutions. It is further validated by simulating con-casting of a 120mm square billet [10].

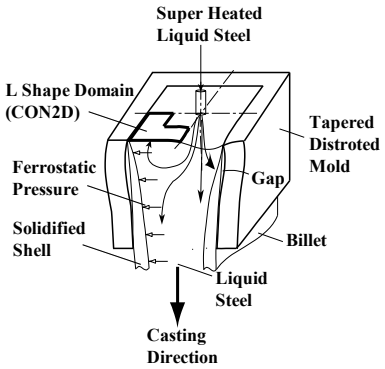

Figure 11. Schematic of billet casting

Heat flux across the inter-face depends on the size of the shrinkage gap, the conductivity of the gap vapor, and the strand roughness. Total heat removal was calibrated to match the measured heatup of the cooling water, as with the CON1D model. Figure 12 shows that the predictions match with thermocouple measurements of mold wall temperature [11]. Figure 13 shows that the model is able to predict shell thickness, including thinning of the corner [11].

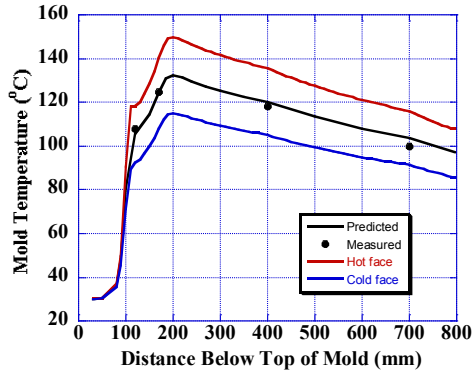

Figure 12 Computed & measured mold temperatures

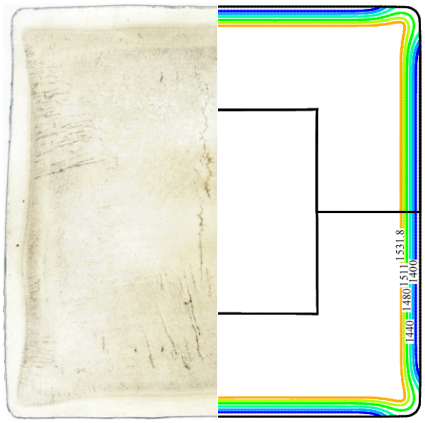

Figure 13: Temperature contours at 285mm below meniscus compared with corresponding sulfur print from plant trial.

4.1 Optimization of mold taper design

One application of the thermal stress model is to optimize mold taper design, especially of the narrow face [12]. Ideal mold taper is affected by thermal shrinkage of the shell, grade-dependent creep strain, and mold distortion. The heat flux profiles for different steel grades and mold fluxes are shown in Figure 14. Peritectic steels have lower heat flux, owing to their deeper oscillation marks, and high-solidification mold fluxes usually used for these grades. As shown in Figure 15, this causes them to have less shrinkage and less taper, in spite of the phase transformation contraction from delta-ferrite to austenite experienced by these steels.

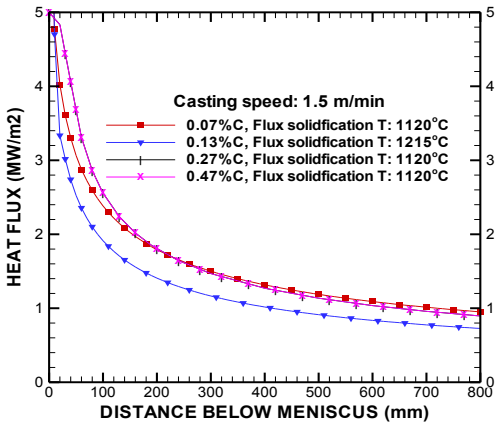

Figure 14: Heat flux profiles for different steel grades (1.5m/min)

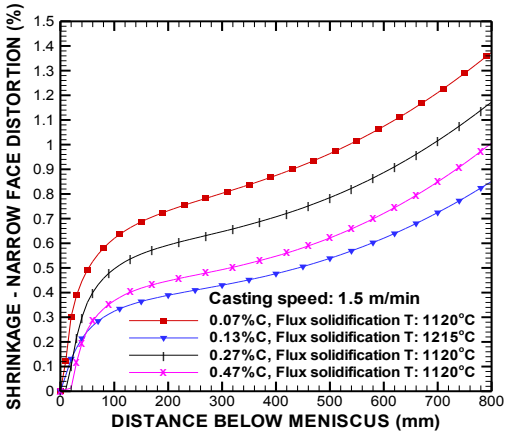

Figure 15: Ideal taper for different steel grades (1.5m/min)

4.2 Maximum casting speed to avoid hot-tear cracks

Another application of the stress model is predicting the maximum casting speed to achieve quality steel at maximum productivity [13]. Casting speed can be limited by factors ranging from excessive level fluctuations, mold friction, insufficient metallurgical length, excessive bulging, reheating in the spray zones and many other problems. One of these is the avoidance of longitudinal cracks, such as the one pictured in Figure 17. Hot-tear cracks are predicted to form when the "damage strain" (tensile strain accumulated at the solidification front within the temperature range between 90 – 99% solid) exceeds a critical value, which depends on steel grade (temperature range across the mushy zone) and strain rate.

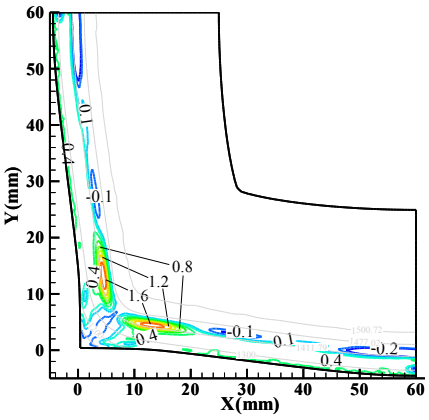

Figure16: Damage Strain Contours at 100mm below Mold Exit (4.4 m/min)

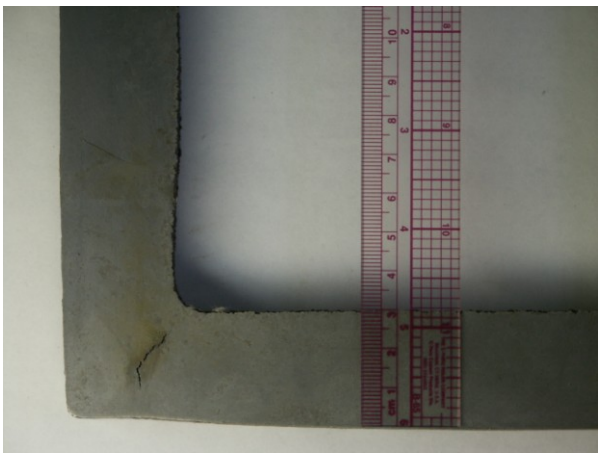

Figure 17: Con-cast billet after breakout showing off-corner sub-surface crack

With increasing casting speed, the shell thickness at mold exit decreases, and the bulging from internal ferrostatic pressure causes corner rotation and tensile strain at the solidification front (Figure 16). The highest damage strains arise at the subsurface off-corner location where the longitudinal cracks are ultimately observed (Figure 17). Casting speed was increased until the maximum damage strain reached the critical value for hot-tear cracks. Results for the critical maximum casting speed were calculated as a function of mold length and section size,[13] assuming ideal mold taper and uniform temperature below mold (ideal spray cooling). Longer molds allow a thicker shell to form, thus increasing the allowable maximum casting speed. Similarly, smaller section sizes experience much less bulging, so can be cast at higher speed. The quantitative ability of the model is demonstrated by comparison with plant measurements. An implication of the model results is that higher casting speed is possible with carefully aligned foot rolls, and by avoiding mold wear. The model can be used for many other practical applications.

6. Acknowledgements

The author thanks the National Science Foundation (Grant DMI-01-15486) and the member companies of the Continuous Casting Consortium at the University of Illinois at Urbana-Champaign (UIUC) for research support. Special thanks are due to graduate students who worked on these projects, including Quan Yuan, Ya Meng, and Chunsheng Li, and to the National Center for Supercomputing Applications (NCSA) at UIUC for computer facilities.

7. References

1. B.G. Thomas, Q. Yuan, L. Zhang, B. Zhao, S.P. Vanka, "Flow Dynamics and Inclusion Transport in Continuous Casting of Steel," in 2004 NSF Design, Service, and Manufacturing Grantees and Research Conf. Proceedings, Southern Methodist Univ, Dallas, TX, (Dallas, TX), 2004, 41p.
2. B.G. Thomas, Q. Yuan, S. Sivaramakrishnan, T. Shi, S.P. Vanka, M.B. Assar, "Comparison of Four Methods to Evaluate Fluid Velocities in CC," ISIJ Internat., Vol. 41 (10), 2001, 1266-1276.
3. Q. Yuan, B.G. Thomas & S.P. Vanka, "Study of Transient Flow and Particle Transport during Continuous Casting of Steel Slabs, I. Fluid Flow," Metall. & Mat. Trans. B, submitted Aug, 2003.
4. Q. Yuan, B.G. Thomas and S.P. Vanka, "Turbulent Flow and Particle Motion in Continuous Slab-Casting Molds," in ISSTech 2003 Process Technology Proceedings, Vol. 86, ISS, Warrendale, PA, (Indianapolis, IN, Apr 27-30, 2003), 2003, 913-927.
5. R.J. O'Malley, personal communication, Middletown, OH, 2003.
6. Q. Yuan, B.G. Thomas & S.P. Vanka, "Study of Transient Flow and Particle Transport during Con. Casting of Steel Slabs, II. Particle Transport," Metal. Mat. Trans. B, accepted Oct, 2003.
7. Y. Meng and B.G. Thomas, "Heat Transfer and Solidification Model of Continuous Slab Casting: CON1D," Metal. & Material Trans., Vol. 34B (5), 2003, 685-705.
8. Y. Meng and B.G. Thomas, "Interfacial Friction-Related Phenomena in Continuous Casting with Mold Slags," in ISSTech 2003 Steelmaking Conf. Proc., Vol. 86, ISS, Warrendale, PA, (Indianapolis, IN, Apr. 27-30, 2003), 2003, 589-606.
9. Y. Kashiwaya, C. Cicutti and A.W. Cramb, "Crystallization Behavior of Mold Slags," in Steelmaking Conf. Proc., Vol. 81, Iron and Steel Soc, Warrendale, PA, 1998, 185-191.
10. C. Li and B.G. Thomas, "Thermo-Mechanical Finite-Element Model of Shell Behavior in Continuous Casting of Steel," Metall. & Materials Trans. B, submitted August, 2003.
11. J.-k. Park, B.G. Thomas and I.V. Samarasekera, "Analysis of Thermo-Mechanical Behavior in Billet Casting with Different Mold Corner Radii," Ironmak. Steelmaking, 29 (5), 2002, 359-375.
12. B.G. Thomas and C. Ojeda, "Ideal Taper Prediction for Slab Casting," in ISSTech 2003 - Manfred Wolf Memorial Symposium Proceedings, Vol. 86, ISS, Warrendale, PA, (Indianapolis, IN, Apr. 27-30, 2003), 2003, 295-308.
13. C. Li and B.G. Thomas, "Maximum Casting Speed for Continuous Cast Steel Billets Based on Sub-Mold Bulging Computation," in Steelmaking Conf. Proc., Vol. 85, ISS, Warrendale, PA, (Nashville, TN, March 10-13, 2002), 2002, 109-130.